

# Optimization and an Investigation on Different Optimum Design Configurations of an Eccentric Twin-Cam Compound Bow

Onur Denizhan<sup>1</sup>, Meng-Sang Chew<sup>2</sup>

<sup>1</sup>Department of Mechanical Engineering, Batman University, Batman, Türkiye

<sup>2</sup>Department of Mechanical Engineering and Mechanics, Lehigh University, Bethlehem, PA, USA

## ARTICLE INFO

### Article History :

Accepted: 08 Feb 2024

Published: 24 Feb 2024

### Publication Issue :

Volume 11, Issue 1

January-February-2024

### Page Number :

291-299

## ABSTRACT

Many patents have been issued for compound bows since they were invented. However, there is just a limited number of research articles on the subject. Besides the dynamics of the compound bow and arrow, the kinematics of the compound bow configuration is significant for the compound bow performance. In this article, an eccentric circular twin-cam compound bow, reported in [7,8] is optimized and several different design configurations of it are investigated. The objective of the optimization in this study is to maximize the stored potential energy at the drawn position. Only three parameters are chosen in this study: the distances between large and small cam geometric centers from the axle, and the angle subtended at the axle between geometric centers of the small and large cams while keeping the main geometry of the compound bow (limb lengths, cam radii and riser length) intact. A total of nine different optimum design configurations are investigated by changing the boundary conditions for the design variables. These are presented and results are discussed.

**Keywords:** Compound Bow, Eccentric Twin-Cam, Optimization, Optimum Design, Potential Energy

## I. INTRODUCTION

The compound bow was first introduced by Allen in 1969 [1]. Since then, many patents for compound bow modifications have been issued. However, research articles on compound bows are limited. A prior study by Bott [2], on optimum design of the compound bow limb (cantilever beam) looks at varying the cross sections and materials for large deflections. Results

show that limbs with a constant cross section and constructed with carbon fiber store more energy. Similar round-wheel compound bow models and design options are also presented by Tiermas [4-6].

A kineto-elastic model of the Banshee twin round-cam compound bow is shown in Fig. 1a. Based on this model, different configurations of this bow will be investigated and optimized. Shown in the figure are

different parts to the compound bow: Riser (grip), upper and lower limbs, string and small and large cams. Note that the elastic deformation of the limb in an actual compound bow is modeled by a torsion spring. All other components shown are assumed inelastic. The compound bow's parameters include limb length, radii of small and large cams, the angle between the geometric centers of these cams, the distance between the axle and the geometric centers of the cams, string length, torsion spring constant, and spring preload or initial angle due to preload.

Based on this model, the objective is to optimize the Banshee compound bow without modifying the main structural geometry of the bow. This results in that only three parameters are available to be optimized among all the aforementioned parameters: Spread angle ( $\sigma$ ) between geometric centers of the small and large cams subtended at the axle point, the large cam offset ( $d$ ) from the axle, and the small cam offset ( $h$ ). Figure 1b shows these three design parameters for the lower cams. The bow is assumed symmetric about the middle axis in this investigation. Note that the large and small cams are not concentric so that the spread angle  $\sigma$  subtended at the axle, is not vanishing.

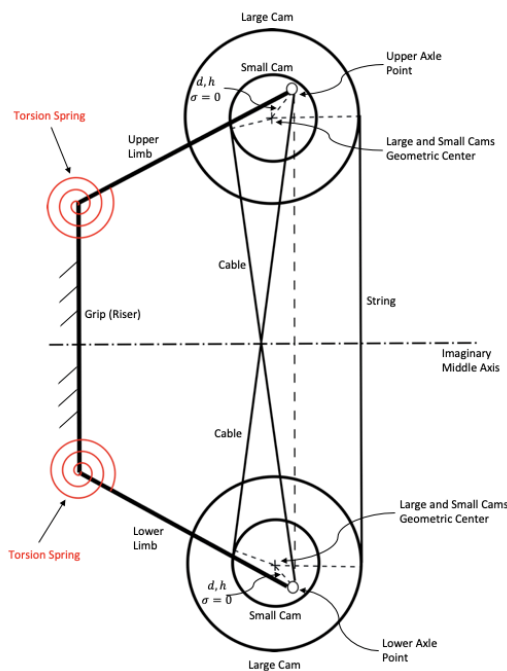


Figure 1a: The compound bow schematic drawing

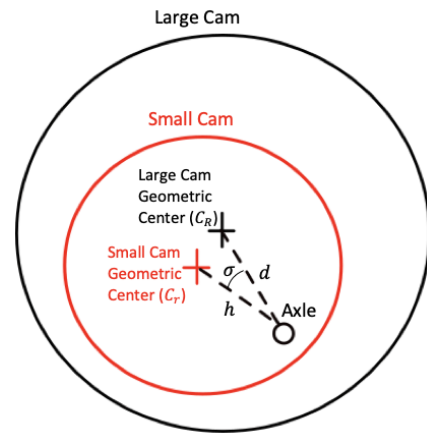


Figure 1b: The compound bow design variables

Based on the three design parameters mentioned above, the objective is to maximize the stored potential energy within the elastic components (torsion springs) in the kineto-elastic model of the Banshee compound bow. The limb length, cam radii and riser length are left unchanged. Nine optimum design configurations resulted. These are presented and results are discussed. In the next section, a kinematic analysis of the bow is presented.

## II. KINEMATIC ANALYSIS

This article focuses on the optimization of the compound bow; therefore, only a summary of the kinematic analysis of the compound bow is provided in this article. For a detailed and systematic kinematic analysis of the twin-cam compound bow the reader is encouraged to look at another article [8] by the authors.

The analysis is performed with following steps:

1. Determine the parametric values of the compound bow at its initial position. This step requires two kinematic vector-loop equations.
2. Calculate the total length of the wrapped cable around the eccentric circular twin-cam. This length is constant even as the bow is drawn. This step requires a total of three equations.

3. Consideration of the wrapped cable length around the twin-cams. Be aware of the shift in the point of the tangency of the cable at the cams. An additional equation is required to determine this wrapped cable length.
4. Determination of the parametric values of the compound bow at the drawn position. This step is required four kinematic vector-loop equations.

Based on these steps; a total of six kinematic vector-loop equations (from Steps 1 and 4) and four other equations (from Steps 2 and 3) are required for a complete kinematic analysis of the eccentric circular twin-cam compound bow.

### III.OPTIMIZATION

One important criterion for the compound bow is the potential energy stored in its limbs, which are modeled by torsion springs at the junctions of the risers and the limbs in this article. If the elastic components store a greater amount of potential energy, the arrow has the capacity to travel a greater distance and achieve higher velocities. On the other hand, it is desirable that the compound bow provides a low peak draw-force (to match the strength of archer) while storing a high level of potential energy. In order to attain the maximum potential energy storage while minimizing draw-force requirements, it is imperative to optimize the design parameters of the compound bow to approximate or attain such a state.

Design parameters of the compound bow eligible for selection as design variables for optimization include: Radii  $R$  and  $r$  of the large or small cams respectively, limb length ( $l_2$ ), torsion spring constant ( $k_s$ ), pre-load magnitude and the initial angle as a result of pre-load ( $\phi_{initial}$ ), the angle between small and large cams geometric centers ( $\sigma$ ), distance between axle point and geometric center of small and large cams ( $h$  and  $d$  respectively), length of the compound bow (string

length ( $s_T$ )). However, in this article, only three parameters are chosen as design variables: The spread angle ( $\sigma$ ) between the eccentricities of the large and small cam; the distances ( $d$ ) and ( $h$ ) between axle point and large cam and small cam geometric centers respectively. The rationale behind selecting solely these three parameters as design variables is to optimize the Banshee compound bow while maintaining the fundamental aspects of the bow geometry, such as limb lengths or cam dimensions, unaltered.

### Optimization Setup

The optimization objective for the compound bow is to maximize the stored potential energy within the bow. Figure 2 shows a plot of the draw-force ( $F_D$ ) vs. draw-length ( $D$ ). Note that the draw force is highly non-linear, and that is due to the kinematics of the cables and the circular twin-cams as a function of the draw. The shaded area under force curve gives the stored potential energy in the compound bow. The let-off point  $D$  is the point where the draw-force is at a minimum and that is where the archer holds before releasing the arrow. For this reason, the area under the draw-force curve only extends until the let-off point.

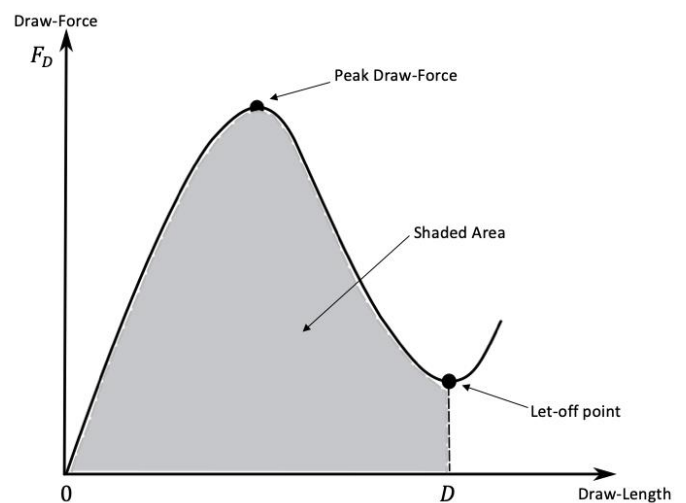


Figure 2: The area under consideration for optimizing the compound bow

In Fig. 2, the shaded region can be determined by computing the definite integral of the draw-force function. Note that the let-off point ( $D$ ) is not constant in the integral because it changes when the parameters (design variables) are being optimized. Note that initially, there is no stored energy at  $O$  even though there is a strain in the limbs of the bow in the initial bow position. This is because at the initial position, the draw-force is zero and so is the draw-length. The torsion springs have a pre-load and therefore, they have initially stored energy but torsion spring parameters are not design variables. Hence, the initially stored potential energy in the torsion springs are held fixed in this study. The upper limit of the stored energy occurs at  $D$  because that is the let-off position where the arrow is released.

Three parameters ( $\sigma$ ,  $h$  and  $d$ ) are chosen as design variables for optimization. Sequential Quadratic Programming (SQP) optimization method is used to solve this nonlinear optimization problem because it ensures the inequality boundary conditions are satisfied in all iterations, and it is faster than the interior point algorithm [9].

The optimization objective can be expressed as follows:

$$\min_{h,d,\sigma} f = - \int_0^D F_D dD$$

subject to (1)

$$\begin{aligned} 0.001 < d < 0.015, \\ 0.001 < h < 0.015, \\ -45^\circ < \sigma < 45^\circ \end{aligned}$$

where  $h$  (m) and  $d$  (m) is the distance between the geometric center of the small and large cams respectively, from the axle point;  $\sigma$  (deg) is the spread angle between the eccentricities of large and small cams;  $F_D$  is the draw-force and displacement  $D$  is the let-off draw-length. Beware that MATLAB *minimizes*

the objective function, so that to maximize an objective function using a MATLAB optimizer, the objective function must be negated [10]. The lower bounds of design variables  $h$  and  $d$  are set to 1 mm instead of zero to prevent these variables from taking zero values. The upper bound of these same variables are chosen to be smaller than the small cam radius so that the axle point is inside of the small cam to be a practical design. The range of the angle  $\sigma$  value is chosen from  $-45^\circ$  to  $45^\circ$ .

The presumed constancy of the stored potential energy by the torsion spring, attributable to its pre-load, is maintained. Based on the experimental determined values determined in [7, 8], the torsion spring initial angle is 0.328 rad to serve as a pre-load and the torsion spring constant ( $k_s$ ) is 145.68 Nm/rad.

### Different Optimum Design Configurations

A total of nine distinct scenarios are examined, each characterized by varying boundary conditions pertaining to the design variables. The torsion springs have pre-load at the initial configuration of the compound bow and as a result of this pre-load, the torsion springs are initially twisted with an initial angle of 0.328 rad. This spring pre-load means that there is initial stored potential energy. To ensure that the main structure of the compound bow is unchanged, this stored potential energy (modeled by the initial twist angle) is therefore fixed for all of the investigated cases. The torsion spring constant ( $k$ ) is 145.6 Nm/rad. These values (initial twist angle and spring constant, modeling the elasticity and pre-load of the actual compound bow limbs, are determined separately from an experiment conducted on the Banshee compound bow [7, 8].

The boundary values of the design variables for each case are shown in Table 1. The spread angle  $\sigma$  is constrained between  $-45^\circ$  and  $45^\circ$ . However, the upper limits on the offset distances  $h$  and  $d$  are

changed depending on the case so as to investigate the compound bow sensitivity to these offset distances. For instance, the boundary values are  $0.002 < h, d < 0.008$  for the Case 1 and are progressively widened to  $0.001 < h, d < 0.015$  for Case 9. Such progressively broadening of the inequality constraints on the offset distances are based on observations from the optimum results in Case 1. Note that lower bounds for these two variables cannot be vanishing. There are no equality constraints in the optimization.

TABLE I  
THE UPPER AND LOWER BOUNDS FOR THE DESIGN VARIABLES

Case No	Boundary Values
1	$0.002 < h, d < 0.008$ $-45^\circ < \sigma < 45^\circ$
2	$0.001 < h, d < 0.008$ $-45^\circ < \sigma < 45^\circ$
3	$0.001 < h, d < 0.009$ $-45^\circ < \sigma < 45^\circ$
4	$0.001 < h, d < 0.010$ $-45^\circ < \sigma < 45^\circ$
5	$0.001 < h, d < 0.011$ $-45^\circ < \sigma < 45^\circ$
6	$0.001 < h, d < 0.012$ $-45^\circ < \sigma < 45^\circ$
7	$0.001 < h, d < 0.013$ $-45^\circ < \sigma < 45^\circ$
8	$0.001 < h, d < 0.014$ $-45^\circ < \sigma < 45^\circ$
9	$0.001 < h, d < 0.015$ $-45^\circ < \sigma < 45^\circ$

#### IV. RESULTS

Figure 3 shows optimum draw-length vs draw-force graph of the optimization. The optimization graph shows that a higher stored potential energy is achieved but with a slightly higher peak draw force. Upon examining the details of the optimized values, a negative value of angle  $\sigma$  is the reason for the higher draw-force at the let-off point. The optimum results

also generally call for a higher value for  $h$  than for  $d$  but both  $h$  and  $d$  values never get close to their respective upper bounds. The lower draw-force value at the let-off point along with a slightly higher peak draw-force results in a significant improvement over the current Banshee compound bow. This is shown in Fig. 3. The optimum values are:  $h = 0.008$  m,  $d = 0.005$  m and  $\sigma = 0.008$  rad with a stored potential energy of 21.5817 J while the original Banshee bow values are:  $h = d = 0.0072$  m and  $\sigma = 0$  rad with a stored potential energy of 21.1782 J. These original Banshee Bow values are presented by Denizhan and Chew [7, 8].

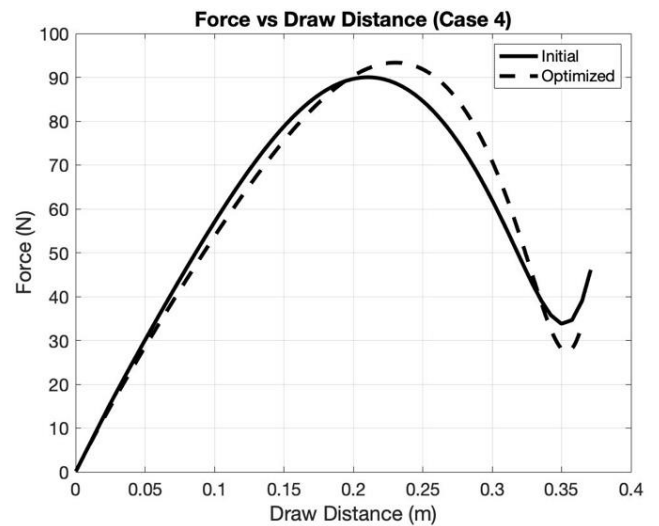


Figure 3: Optimum draw-length vs draw-force graph

Tables 2, 3 and 4 show optimum results of the design variables ( $\sigma, h$  and  $d$ ) along with the other parameters: The largest draw-force value  $F_{max}$ , the lowest draw-force value  $F_{LO}$  (at the let-off point), the limb angular displacement at let-off point ( $\Delta\phi$ ) and the area under the draw force curve at the let-off point. In these tables,  $C_R$  and  $C_r$  the large and small cams geometric centers, respectively. The Point  $E$  refers the axle point of the cams and it is located at the same point for both cams, which are fixed relative to each other. To conform to table/page size requirements, three tables are used, with each summarizing three cases. Therefore, Cases 1, 2 and 3 are shown in Table 2, Cases 4, 5 and 6 in Table

3, and Cases 7, 8 and 9 in Table 4. The first column in these tables show the values for the initial configuration of the cams which is that based on the Banshee compound bow. The third column shows the optimum numerical results with along with figures of the optimum cam configurations. The last column shows the resulting draw-force vs draw displacement curves (dashed). For comparison the initial design draw-force vs draw displacement curves are shown (solid).

Table 2 shows the optimum results for Cases 1, 2 and 3. The geometric centers of the small and large cams  $C_r$  and  $C_R$  are initially located at the same point (concentric). In the optimized cases, the geometric centers of the small and large cams are not concentric. The optimum angle  $\sigma$  is near zero in all these cases which is reflect in the draw-force curve fluctuation having a similar variation as compared to the initial case (concentric). Case 3 has the highest stored potential energy even though the associated let-off force and peak draw-force are the lowest among these three cases. Since the optimum variable  $h$  (small cam offset) is the same in these three cases, the differences in the let-off forces and peak draw-forces between the three cases show that these forces are most sensitive to  $d$  (large cam offset) and  $\sigma$ . Furthermore, the optimum draw distance in all Cases 1, 2 and 3 remain unchanged from the initial values.

The optimum results for Cases 4, 5 and 6 are shown in the Table 3. Case 4 is the optimum configuration that has the lowest let-off force between these three cases. However, it also has the lowest stored potential energy.

Case 6 has the lowest and Case 5 has the highest peak draw-force while the optimum let-off forces for these two cases are very nearly the same. Furthermore, in contrast to Case 4, the optimum angle  $\sigma$  values are negative for Cases 5 and 6. A comparison in the other design variables between the cases, shows that the reason for the low fluctuation in draw-force curve can be attributed to the negative  $\sigma$  values that also result in Cases 5 and 6 have longer draw distances as compared to the initial design.

Table 4 shows the optimum results of the Cases 7, 8 and 9. Case 9 has the lowest let-off force and the highest stored potential energy among these three cases. While Case 8 has the highest peak draw-force, Case 7 has the lowest peak draw-force among these three cases. Similar with Cases 5 and 6, Cases 7, 8 and 9 have the negative optimum angle  $\sigma$  values. Therefore, the draw-force fluctuation is small in much the same manner as Cases 5 and 6. The optimum draw distance is longer than initial design for all the Cases 7, 8 and 9.

From a closer examination of Tables 2, 3 and 4, the optimum draw-forces that are very similar to the initial design of the compound bow are in Cases 3 and 4. Moreover, the optimum let-off forces for these two cases are lower, and the peak forces are just a few newtons higher than the initial design values while the draw distances remain unchanged from the initial design. The optimum of the compound bow limb rotation angles ( $\Delta\phi$ ) for all cases change very minimally from the initial which means that ( $\Delta\phi$ ) is not sensitive to the design variables ( $\sigma$ ,  $h$  and  $d$ ).

TABLE 2. OPTIMIZED CASES 1, 2 AND 3

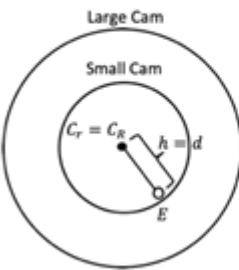
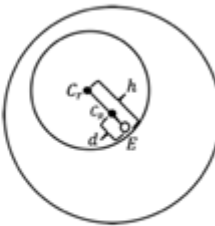
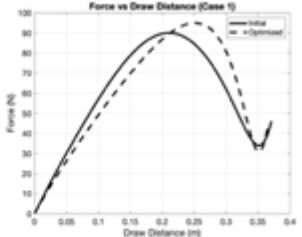
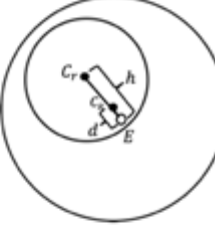
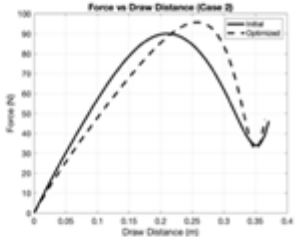
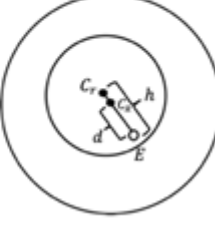
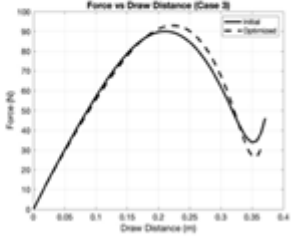
Initial Configuration	Case No	Optimum Configurations and Optimization Results	Draw-Force vs Draw Distance Graphs																												
<p>Large Cam</p> <p>Small Cam</p> <p><math>C_r = C_R</math> <math>h = d</math></p>  <table border="1" data-bbox="263 705 502 896"> <tr><td><math>h</math></td><td>0.0072</td></tr> <tr><td><math>\sigma</math></td><td>0</td></tr> <tr><td><math>d</math></td><td>0.0072</td></tr> <tr><td>Area(P.E.)</td><td>21.1782</td></tr> <tr><td><math>\Delta\phi</math></td><td>0.2359</td></tr> <tr><td><math>F_{max}</math></td><td>90.0126</td></tr> <tr><td><math>F_{LO}</math></td><td>33.6991</td></tr> </table>	$h$	0.0072	$\sigma$	0	$d$	0.0072	Area(P.E.)	21.1782	$\Delta\phi$	0.2359	$F_{max}$	90.0126	$F_{LO}$	33.6991	1	 <table border="1" data-bbox="837 280 1021 481"> <tr><td><math>h</math></td><td>0.008</td></tr> <tr><td><math>\sigma</math></td><td>0.027</td></tr> <tr><td><math>d</math></td><td>0.002</td></tr> <tr><td>Area</td><td>21.4513</td></tr> <tr><td><math>\Delta\phi</math></td><td>0.2383</td></tr> <tr><td><math>F_{max}</math></td><td>94.9854</td></tr> <tr><td><math>F_{LO}</math></td><td>30.8165</td></tr> </table>	$h$	0.008	$\sigma$	0.027	$d$	0.002	Area	21.4513	$\Delta\phi$	0.2383	$F_{max}$	94.9854	$F_{LO}$	30.8165	
	$h$	0.0072																													
	$\sigma$	0																													
	$d$	0.0072																													
	Area(P.E.)	21.1782																													
	$\Delta\phi$	0.2359																													
	$F_{max}$	90.0126																													
	$F_{LO}$	33.6991																													
	$h$	0.008																													
$\sigma$	0.027																														
$d$	0.002																														
Area	21.4513																														
$\Delta\phi$	0.2383																														
$F_{max}$	94.9854																														
$F_{LO}$	30.8165																														
2	 <table border="1" data-bbox="837 526 1021 728"> <tr><td><math>h</math></td><td>0.008</td></tr> <tr><td><math>\sigma</math></td><td>0.038</td></tr> <tr><td><math>d</math></td><td>0.001</td></tr> <tr><td>Area</td><td>21.3732</td></tr> <tr><td><math>\Delta\phi</math></td><td>0.2376</td></tr> <tr><td><math>F_{max}</math></td><td>95.7139</td></tr> <tr><td><math>F_{LO}</math></td><td>32.0962</td></tr> </table>	$h$	0.008	$\sigma$	0.038	$d$	0.001	Area	21.3732	$\Delta\phi$	0.2376	$F_{max}$	95.7139	$F_{LO}$	32.0962																
$h$	0.008																														
$\sigma$	0.038																														
$d$	0.001																														
Area	21.3732																														
$\Delta\phi$	0.2376																														
$F_{max}$	95.7139																														
$F_{LO}$	32.0962																														
3	 <table border="1" data-bbox="837 772 1021 974"> <tr><td><math>h</math></td><td>0.008</td></tr> <tr><td><math>\sigma</math></td><td>0.008</td></tr> <tr><td><math>d</math></td><td>0.006</td></tr> <tr><td>Area</td><td>21.5816</td></tr> <tr><td><math>\Delta\phi</math></td><td>0.2396</td></tr> <tr><td><math>F_{max}</math></td><td>92.9818</td></tr> <tr><td><math>F_{LO}</math></td><td>26.4452</td></tr> </table>	$h$	0.008	$\sigma$	0.008	$d$	0.006	Area	21.5816	$\Delta\phi$	0.2396	$F_{max}$	92.9818	$F_{LO}$	26.4452																
$h$	0.008																														
$\sigma$	0.008																														
$d$	0.006																														
Area	21.5816																														
$\Delta\phi$	0.2396																														
$F_{max}$	92.9818																														
$F_{LO}$	26.4452																														

TABLE 3. OPTIMIZED CASES 4, 5 AND 6

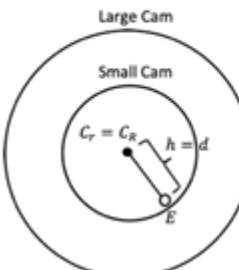
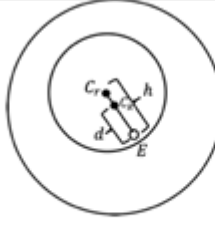
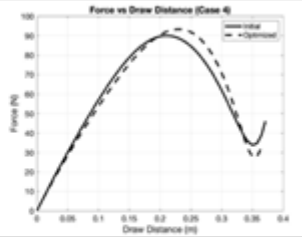
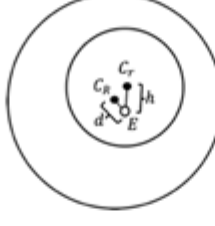
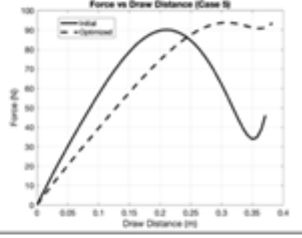
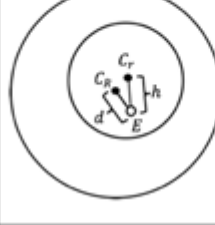
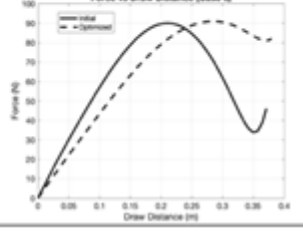
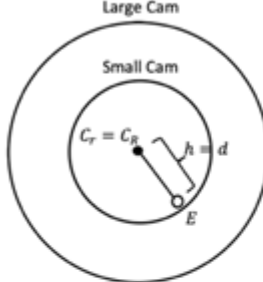
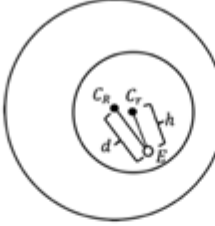
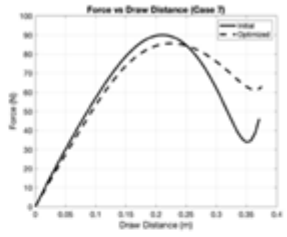
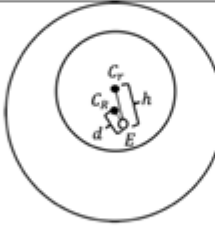
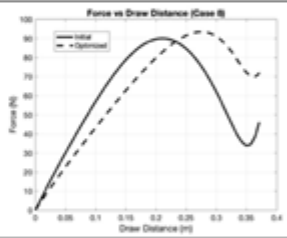
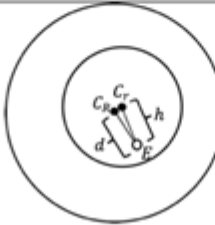
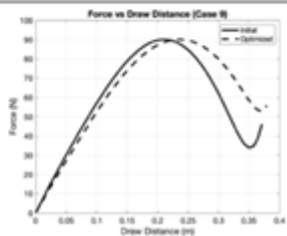
Initial Configuration	Case No	Optimum Configurations and Optimization Results	Draw-Force vs Draw Distance Graphs																												
<p>Large Cam</p> <p>Small Cam</p> <p><math>C_r = C_R</math> <math>h = d</math></p>  <table border="1" data-bbox="263 1534 502 1724"> <tr><td><math>h</math></td><td>0.0072</td></tr> <tr><td><math>\sigma</math></td><td>0</td></tr> <tr><td><math>d</math></td><td>0.0072</td></tr> <tr><td>Area(P.E.)</td><td>21.1782</td></tr> <tr><td><math>\Delta\phi</math></td><td>0.2359</td></tr> <tr><td><math>F_{max}</math></td><td>90.0126</td></tr> <tr><td><math>F_{LO}</math></td><td>33.6991</td></tr> </table>	$h$	0.0072	$\sigma$	0	$d$	0.0072	Area(P.E.)	21.1782	$\Delta\phi$	0.2359	$F_{max}$	90.0126	$F_{LO}$	33.6991	4	 <table border="1" data-bbox="837 1131 1021 1332"> <tr><td><math>h</math></td><td>0.008</td></tr> <tr><td><math>\sigma</math></td><td>0.008</td></tr> <tr><td><math>d</math></td><td>0.005</td></tr> <tr><td>Area</td><td>21.5817</td></tr> <tr><td><math>\Delta\phi</math></td><td>0.2397</td></tr> <tr><td><math>F_{max}</math></td><td>93.3293</td></tr> <tr><td><math>F_{LO}</math></td><td>27.4623</td></tr> </table>	$h$	0.008	$\sigma$	0.008	$d$	0.005	Area	21.5817	$\Delta\phi$	0.2397	$F_{max}$	93.3293	$F_{LO}$	27.4623	
	$h$	0.0072																													
	$\sigma$	0																													
	$d$	0.0072																													
	Area(P.E.)	21.1782																													
	$\Delta\phi$	0.2359																													
	$F_{max}$	90.0126																													
	$F_{LO}$	33.6991																													
	$h$	0.008																													
$\sigma$	0.008																														
$d$	0.005																														
Area	21.5817																														
$\Delta\phi$	0.2397																														
$F_{max}$	93.3293																														
$F_{LO}$	27.4623																														
5	 <table border="1" data-bbox="837 1377 1021 1579"> <tr><td><math>h</math></td><td>0.003</td></tr> <tr><td><math>\sigma</math></td><td>-0.785</td></tr> <tr><td><math>d</math></td><td>0.001</td></tr> <tr><td>Area</td><td>22.1150</td></tr> <tr><td><math>\Delta\phi</math></td><td>0.2445</td></tr> <tr><td><math>F_{max}</math></td><td>93.7574</td></tr> <tr><td><math>F_{LO}</math></td><td>90.7822</td></tr> </table>	$h$	0.003	$\sigma$	-0.785	$d$	0.001	Area	22.1150	$\Delta\phi$	0.2445	$F_{max}$	93.7574	$F_{LO}$	90.7822																
$h$	0.003																														
$\sigma$	-0.785																														
$d$	0.001																														
Area	22.1150																														
$\Delta\phi$	0.2445																														
$F_{max}$	93.7574																														
$F_{LO}$	90.7822																														
6	 <table border="1" data-bbox="837 1624 1021 1825"> <tr><td><math>h</math></td><td>0.004</td></tr> <tr><td><math>\sigma</math></td><td>-0.785</td></tr> <tr><td><math>d</math></td><td>0.003</td></tr> <tr><td>Area</td><td>23.2424</td></tr> <tr><td><math>\Delta\phi</math></td><td>0.2549</td></tr> <tr><td><math>F_{max}</math></td><td>90.9940</td></tr> <tr><td><math>F_{LO}</math></td><td>81.0697</td></tr> </table>	$h$	0.004	$\sigma$	-0.785	$d$	0.003	Area	23.2424	$\Delta\phi$	0.2549	$F_{max}$	90.9940	$F_{LO}$	81.0697																
$h$	0.004																														
$\sigma$	-0.785																														
$d$	0.003																														
Area	23.2424																														
$\Delta\phi$	0.2549																														
$F_{max}$	90.9940																														
$F_{LO}$	81.0697																														

TABLE 4. OPTIMIZED CASES 7, 8 AND 9

Initial Configuration	Case No	Optimum Configurations and Optimization Results	Draw-Force vs Draw Distance Graphs																												
 <table border="1" data-bbox="255 705 486 896"> <tr><td><math>h</math></td><td>0.0072</td></tr> <tr><td><math>\sigma</math></td><td>0</td></tr> <tr><td><math>d</math></td><td>0.0072</td></tr> <tr><td><math>Area(P.E.)</math></td><td>21.1782</td></tr> <tr><td><math>\Delta\phi</math></td><td>0.2359</td></tr> <tr><td><math>F_{max}</math></td><td>90.0126</td></tr> <tr><td><math>F_{LO}</math></td><td>33.6991</td></tr> </table>	$h$	0.0072	$\sigma$	0	$d$	0.0072	$Area(P.E.)$	21.1782	$\Delta\phi$	0.2359	$F_{max}$	90.0126	$F_{LO}$	33.6991	7	 <table border="1" data-bbox="837 302 1029 504"> <tr><td><math>h</math></td><td>0.005</td></tr> <tr><td><math>\sigma</math></td><td>-0.488</td></tr> <tr><td><math>d</math></td><td>0.007</td></tr> <tr><td><math>Area</math></td><td>22.5694</td></tr> <tr><td><math>\Delta\phi</math></td><td>0.2487</td></tr> <tr><td><math>F_{max}</math></td><td>85.5613</td></tr> <tr><td><math>F_{LO}</math></td><td>61.2414</td></tr> </table>	$h$	0.005	$\sigma$	-0.488	$d$	0.007	$Area$	22.5694	$\Delta\phi$	0.2487	$F_{max}$	85.5613	$F_{LO}$	61.2414	
	$h$	0.0072																													
	$\sigma$	0																													
$d$	0.0072																														
$Area(P.E.)$	21.1782																														
$\Delta\phi$	0.2359																														
$F_{max}$	90.0126																														
$F_{LO}$	33.6991																														
$h$	0.005																														
$\sigma$	-0.488																														
$d$	0.007																														
$Area$	22.5694																														
$\Delta\phi$	0.2487																														
$F_{max}$	85.5613																														
$F_{LO}$	61.2414																														
8	 <table border="1" data-bbox="837 548 1029 750"> <tr><td><math>h</math></td><td>0.005</td></tr> <tr><td><math>\sigma</math></td><td>-0.356</td></tr> <tr><td><math>d</math></td><td>0.001</td></tr> <tr><td><math>Area</math></td><td>22.3616</td></tr> <tr><td><math>\Delta\phi</math></td><td>0.2467</td></tr> <tr><td><math>F_{max}</math></td><td>93.4362</td></tr> <tr><td><math>F_{LO}</math></td><td>69.9047</td></tr> </table>	$h$	0.005	$\sigma$	-0.356	$d$	0.001	$Area$	22.3616	$\Delta\phi$	0.2467	$F_{max}$	93.4362	$F_{LO}$	69.9047																
$h$	0.005																														
$\sigma$	-0.356																														
$d$	0.001																														
$Area$	22.3616																														
$\Delta\phi$	0.2467																														
$F_{max}$	93.4362																														
$F_{LO}$	69.9047																														
9	 <table border="1" data-bbox="837 784 1029 985"> <tr><td><math>h</math></td><td>0.006</td></tr> <tr><td><math>\sigma</math></td><td>-0.406</td></tr> <tr><td><math>d</math></td><td>0.006</td></tr> <tr><td><math>Area</math></td><td>23.2280</td></tr> <tr><td><math>\Delta\phi</math></td><td>0.2547</td></tr> <tr><td><math>F_{max}</math></td><td>90.0202</td></tr> <tr><td><math>F_{LO}</math></td><td>53.0895</td></tr> </table>	$h$	0.006	$\sigma$	-0.406	$d$	0.006	$Area$	23.2280	$\Delta\phi$	0.2547	$F_{max}$	90.0202	$F_{LO}$	53.0895																
$h$	0.006																														
$\sigma$	-0.406																														
$d$	0.006																														
$Area$	23.2280																														
$\Delta\phi$	0.2547																														
$F_{max}$	90.0202																														
$F_{LO}$	53.0895																														

V. DISCUSSION

The varying draw-force function and the force at the let-off point are important characteristics of a compound bow. The optimizer has been successful in determining the best combination of the three parameters,  $h$ ,  $d$  and  $\sigma$  that maximizes the stored energy of the bow while reducing the force at the let-off point which only a small increase in the peak draw force.

The cases show that optimum cases generally tend to have larger  $h$  value (small cam offset) than  $d$  (large cam offset) because the optimum  $h$  value is always larger than that for  $d$  except in Cases 7 and 9. The results also show that the optimum cases tend to have the lowest  $d$  and  $h$  values.

Case 3 and Case 4 can be one of the best optimum designs since they have low draw-forces at the let-off point with only a small increase in the peak draw-force compared to the initial design values. The rest of the

design variable values and the stored potential energies for both cases are almost identical.

As the bounds of the two cam offsets are loosened, the optimum designs become better so that Cases 3 and 4 give excellent results. The other cases are comparable. This is due to two reasons: The first is that the optimization procedure with loosened bounds on the design variables, is able to converge into other local optimum solutions. If a global optimization procedure is used, the subsequent cases either should remain the same or gets better. The other reason is that the optimization criterion given by Eq. (1) does not include some of the characteristics that are important in our final judgment on what constitute as the best solution. Characteristics such as low let-off force and low peak draw-force. What is needed is a multi-objective criterion that penalizes the let-off force and peak draw-force while maximizing the energy stored in the compound bow up to the point of let-off. This is a subject worthy of further study.



The findings also suggest that a negative angle  $\sigma$  could potentially explain the elevated draw force observed at the let-off point, minimized draw force variability, and an extended draw distance. The stored potential energy is higher than the original configuration in all nine cases. However, it is important to note that just because a case is optimum does not mean that the design configurations is practical. It is always important to go back and check for practicality.

## VI. CONCLUSION

In this article, an optimization of the eccentric twin-cam compound bow is introduced and optimum results from total of nine different design configurations of the compound bow are presented and discussed. The purpose is to maximize the stored potential energy within the compound bow while the least changes to the Banshee compound bow. Without changing the main parts of the Banshee compound bow, significant improvements have been found possible just by adjusting only the parameters of the cams. The results show that two of the configurations are optimal and are practical.

## VII. REFERENCES

- [1] Allen, H. W. Archery bow with draw force multiplying attachments. USA, Mo. Patent 3,486,495. 1969. <https://patents.google.com/patent/US3486495A/en>
- [2] Bott, S. Optimal design of the limb in compound bows. M.Sc. thesis, University of Missouri-Columbia, USA, 2019. <https://mospace.umsystem.edu/xmlui/handle/10355/72270>
- [3] Denizhan, O., Chew, MS. "Optimum Design of an Archery Twin Round-Wheel Compound Bow." *Proceedings of the ASME 2020 International Design Engineering Technical Conferences and Computers and Information in Engineering Conference. Volume 10: 44th Mechanisms and Robotics Conference (MR)*. Virtual, Online. August 17–19, 2020. V010T10A027. ASME. <https://doi.org/10.1115/DETC2020-22473>
- [4] Tiermas, M. An advanced model of the round-wheel compound bow. *Meccanica* 51, 1201–1207 (2016). <https://doi.org/10.1007/s11012-015-0262-5>
- [5] Tiermas, M. A model of the twin-cam compound bow with cam design options. *Meccanica* 52, 421–429 (2017). <https://doi.org/10.1007/s11012-016-0395-1>
- [6] Tiermas, M. The round-wheel compound bow model revisited: a new extension. *Sports Eng* 20, 155–162 (2017). <https://doi.org/10.1007/s12283-017-0225-2>
- [7] Denizhan, O. Incorporation of kinematic analysis, synthesis and optimization into static balancing. Ph.D. thesis, USA, Lehigh University, (2021). <https://www.proquest.com/docview/2580344031?pq-origsite=gscholar&fromopenview=true&sourcetype=Dissertations%20&%20Theses>
- [8] Denizhan, O. and Chew, MS. A systematic kinematic analysis and experimental verification of an eccentric twin-cam compound bow. *Proceedings of the Institution of Mechanical Engineers, Part C: Journal of Mechanical Engineering Science (Under review)*.
- [9] Venkataraman, P. Applied optimization with MATLAB programming. 2<sup>nd</sup> edition, *Wiley Publishing*, (2009). <https://www.wiley.com/en-sg/exportProduct/pdf/9780470084885>
- [10] Global optimization toolbox release notes. *The MathWorks, Inc.*, March 2021 (R2021a) edition, (2021). <https://www.mathworks.com/help/gads/release-notes.html>

### Cite this article as :

Onur Denizhan, Meng-Sang Chew, "Optimization and an Investigation on Different Optimum Design Configurations of an Eccentric Twin-Cam Compound Bow", *International Journal of Scientific Research in Science, Engineering and Technology (IJSRSET)*, Online ISSN : 2394-4099, Print ISSN : 2395-1990, Volume 11 Issue 1, pp. 291-299, January-February 2024. Available at doi : <https://doi.org/10.32628/IJSRSET2411144>  
Journal URL : <https://ijsrset.com/IJSRSET2411144>